3D SIMULATION OF A 500 KG UO_2 MELT IN A COLD CRUCIBLE INDUCTION FURNACE

E. Sauvage[1], *P. Brun*[1], *J. Lacombe*[1], *L. Aufore*[2]

[1] *CEA Marcoule, DEN, DTCD, SCDV, LDPV, F-30207, Bagnols-sur-Cze*
[2] *CEA Cadarache, DEN, DTN, SMTA, F-13115, St Paul-les-Durance*
e-Mail: Emilien.Sauvage@cea.fr

In the field of severe accident studies for nuclear generation reactors 2, 3 and 4, the Plinius-2 project aims to build a new facility to perform experiments of corium interactions tests at a large scale until 2020. In this context, the project in collaboration with ECM Technology has to define and build a furnace able to melt up to 500 kg of simulated corium of various compositions (mix of UO_2, ZrO_2, steel or concrete). The work presented in this article is a 3D dimensional simulation of a large load of UO_2 melts in a cold crucible, including turbulence modelling, induction heating and stirring. Solidification of the oxide near the cold wall of the crucible is taken into account as well as the heat radiation transfer at the free surface.

Introduction. The cold crucible technology has been selected in this project because it has already proven his ability to melt corium thanks to Korean [1, 2] and Russian [3, 4] works but only for lower mass. Simulation of such induction furnace is quite well known in the CEA Marcoule for vitrifiction purposes [5, 6]. But the simulation has to be upgraded to take into account LES turbulence modelling and Lorentz forces which were both neglected for glass simulations due to its very high viscosity and low electrical conductivity. Recent work [7] demonstrates the feasibility of similar simulation using a LES turbulence model with a very good accuracy.

1. Presentation of the problem. The simulation is performed with (i) the Ansys–Fluent software for fluid mechanics and thermal equations and (ii) the Flux software (Cedrat) for the inductive part. The Flux software has been chosen because of its good ability to solve large domains with a strong spatial variation of the electrical conductivity. Moreover, it has been used in our laboratory for a long enough time in purely inductive problems. The coupling between the two softwares is based on automatic file transfers and first order interpolation between the two meshes.

1.1. Geometry. The load is a simple cylinder of 500 mm in diameter and 400 mm high, which represents a load of around 550 kg of UO_2. Fig. 1 shows the computation domain for the induction computation and for the fluid mechanism part. The mesh size of the fluid domain in Fluent is about 1 million with a boundary layer near all walls. The maximum mesh size is about 5 mm. The time step resolution is 0.001 s to have a Courant number less than unity in all the domain.

1.2. Physical properties. The physical properties of UO_2 (viscosity, density, heat capacity and thermal conductivity) come from [8] and the electrical conductivity from [9]. The values used in the present work are summarize in Table 1. Note that the density, viscosity and electrical conductivity are functions of the temperature.

1.3. Induction modelling. The magnetic Reynolds number $\mathrm{Rm} = \mu_0 \sigma R U$ is estimated, in our case, by the electrical conductivity of UO_2 in the liquid state

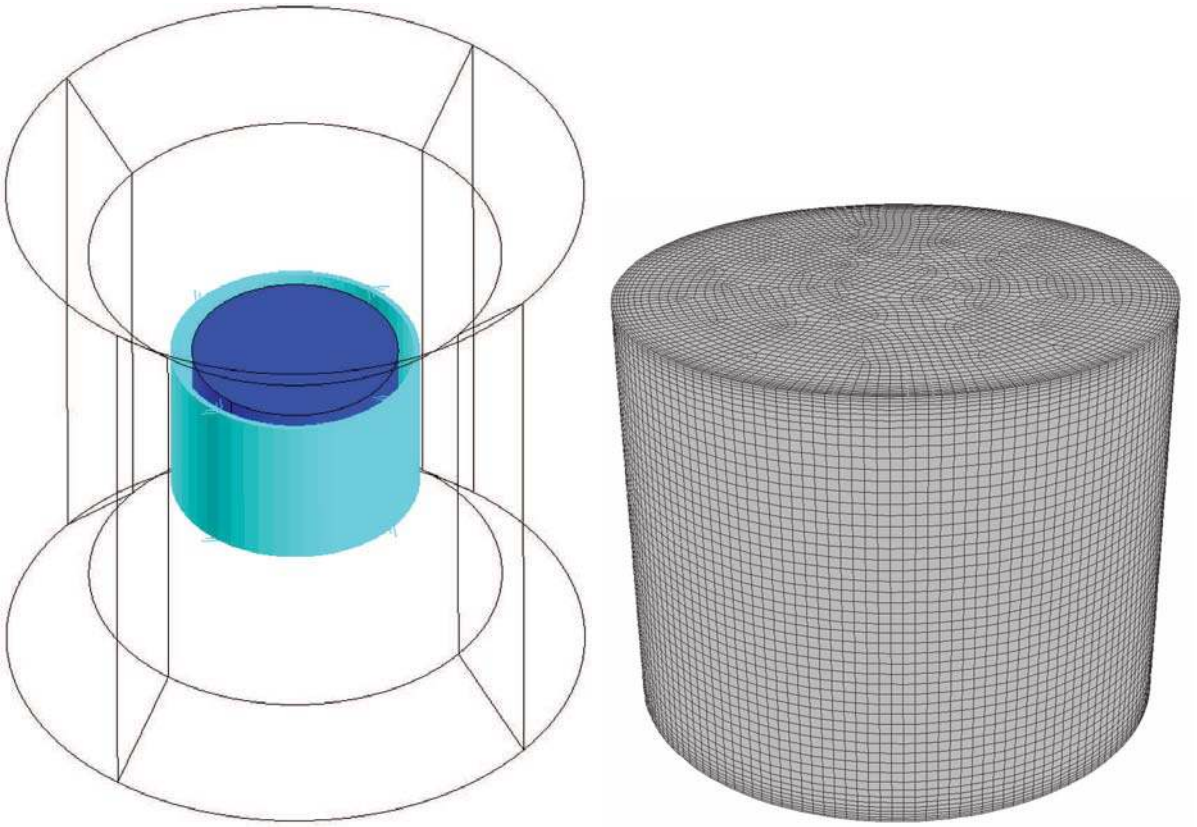

(*a*) (*b*)

Fig. 1. View of the computation domain. (*a*) In Flux software;(*b*) In Fluent software.

Table 1. Physical properties of UO_2 used in this work (T stands for the temperature in K.)

Properties	Symbol	Unit	Value/Law
Density	ρ	$\mathrm{kgm^{-3}}$	10900–0.7
Heat capacity	C_p	$\mathrm{Jkg^{-1}K^{-1}}$	480
Thermal conductivity	λ	$\mathrm{W\,m^{-1}K^{-1}}$	9
Viscosity	μ	$\mathrm{kgm^{-1}s^{-1}}$	$T > 3120\mathrm{K} : 0.004$ and $T < 3120\mathrm{K} : 10^4$
Electrical conductivity	σ	$\mathrm{\Omega^{-1}m^{-1}}$	$3.569{\cdot}10^5\,\mathrm{e}^{-13345/T}$

($T = 3500\,\mathrm{K}$) combined with a maximum velocity of $0.1\,\mathrm{m/s}$ and a characteristic length of $0.5\,\mathrm{m}$. A value of $\mathrm{Rm} < 10^{-3}$ is found, implying that the standard Ohm's law $\mathbf{j} = \sigma\mathbf{E}$ is valid with the electrical current density $\mathbf{j}\,[\mathrm{Am^{-2}}]$ and the vector electric field $\mathbf{E}\,[\mathrm{V/m}]$. Moreover, the material is assumed to be non-magnetic. The classical induction equation is solved in the $\mathbf{A}$-V formalism, where $\mathbf{A}\,[\mathrm{Tm}]$ is the potential vector magnetic and $V\,[\mathrm{V}]$ is the scalar potential under the magneto-quasistatic approximation in complex notation:

$$\boldsymbol{\nabla} \wedge \left(\frac{1}{\mu_0} \boldsymbol{\nabla} \wedge \mathbf{A} \right) + \sigma \left(\imath\omega\mathbf{A} + \boldsymbol{\nabla} V \right) = \mathbf{0}, \tag{1}$$

$$\boldsymbol{\nabla} \cdot \left(\sigma \left(\imath\omega\mathbf{A} + \boldsymbol{\nabla} V \right) \right) = \mathbf{0}, \tag{2}$$

where $\mu_0\,[\mathrm{H/m}]$ is the vacuum permeability, $\imath$ is the imaginary number, and $\omega\,[\mathrm{rad/s}]$ is the angular frequency.

The commercial software Flux is used to solve induction equations with the electrical conductivity as a function of the temperature. The crucible as well the inductor are not modelled, they are approximated by a current sheet around the glass, as seen in Fig. 1*a*. In this coil, an alternating current ($I_{\mathrm{eff}} = 1500\,\mathrm{A}$ and $f = 100\,\mathrm{kHz}$) is imposed.

1.4. Flow modelling. The Navier–Stokes equations for incompressible flow are solved in the Fluent software. The Reynolds number $\mathrm{Re} = \rho U L/\mu$ is about 10^5 ($U = 0.1\,\mathrm{m/s}$, $L = 0.5\,\mathrm{m}$) which signifies that a turbulence model is required. Large Eddy Simulation (LES) modelling is used in this work meaning that large scales are fully solved, whereas small scales are modelled. The equations after the spatial filtering process are shown, one can note the presence of the Lorentz force term with $\mathbf{u}\,[\mathrm{m/s}]$ as the velocity vector and $p\,[\mathrm{Pa}]$ as the pressure:

$$\boldsymbol{\nabla} \cdot \mathbf{u} = 0, \tag{3}$$

$$\rho \left(\frac{\partial \mathbf{u}}{\partial t} + (\mathbf{u} \cdot \boldsymbol{\nabla})\, \mathbf{u} \right) = - \boldsymbol{\nabla} p + \boldsymbol{\nabla} \cdot \left((\mu + \mu_\mathrm{t}) \left(\boldsymbol{\nabla} \mathbf{u} + \boldsymbol{\nabla} \mathbf{u}^T \right) \right) + \rho \mathbf{g} + \frac{1}{2} \Re\mathrm{e} \left\{ \mathbf{j} \wedge \mathbf{B}^* \right\}, \tag{4}$$

where μ_t is the subgrid-scale turbulent viscosity defined by the choice of the subgrid-scale turbulence model. In this work, we use the Smagorinsky-Lilly model [10], as described in the Fluent documentation. The thermal equation is solved with a source term due the Joule power losses related to the induction equation:

$$\rho C_p \left(\frac{\partial T}{\partial t} + (\mathbf{u} \cdot \boldsymbol{\nabla})\, T \right) = \boldsymbol{\nabla} \cdot \left((\lambda + \lambda_\mathrm{t})\, \boldsymbol{\nabla} T \right) + \frac{j j^*}{2\sigma}, \tag{5}$$

where λ_t is the turbulent thermal conductivity related to the subgrid-scale turbulent viscosity, as defined in the Smagorinsky–Lilly model [10].

1.5. Boundary conditions. The side and bottom part of the load are in contact with the cold crucible. In this study, for first simulation, we will neglect the thermal resistance between the load and the cold surface. Further work will be necessary to take it into account. The perfect contact is modelled with a Dirichlet condition $T_\mathrm{w} = 800\,\mathrm{K}$ associated with a non-slip condition $\mathbf{u} = \mathbf{0}$. At the free surface, a thermal radiation condition is set: $\phi = \sigma_\mathrm{sb} \epsilon \left(T_\mathrm{w}^4 - T_\mathrm{ref}^4 \right)$ with $\epsilon = 0.6$ and $T_\mathrm{ref} = 1000\,\mathrm{K}$.

1.6. Coupling software. The main issue is to couple a finite element and a volume finite based software. Moreover, mesh refinement requirements are different for the induction and hydrodynamic phenomena. Consequently, using a unique mesh is not possible and data transfers between the two meshes are necessary. The coupling is based on interpolations and data files transfers. Each software interpolates the chosen field on the computing nodes of the other software. A C-shell script supervises the two softwares and launches them when the other is done. The general algorithm is shown in Fig. 2.

As a first step, each software reads and keeps in memory the computing nodes of the other software. Then, when the Fluent computation is over, it does a first order interpolation of the temperature value on Flux nodes using the temperature and the gradient of the temperature value of the cell center. Due to these prelocalizations, the transfer times are negligible if compared with the convergence time of Flux or Fluent. Moreover, this coupling performs an accurate interpolation between the two computational grids, so very small losses of precision are to be notified.

2. Results and discussion. Fig. 3 shows some results of the computation with an imposed total Joule power in a load of 1.2 MW. The intial conditions were the uniform temperature $T = 2800\,\mathrm{K}$ and $\mathbf{u} = \mathbf{0}$. Almost 2000 s of the physical time were necessary to obtain a thermal stabilization between the amount of the injected power and the power received by the cooled walls.

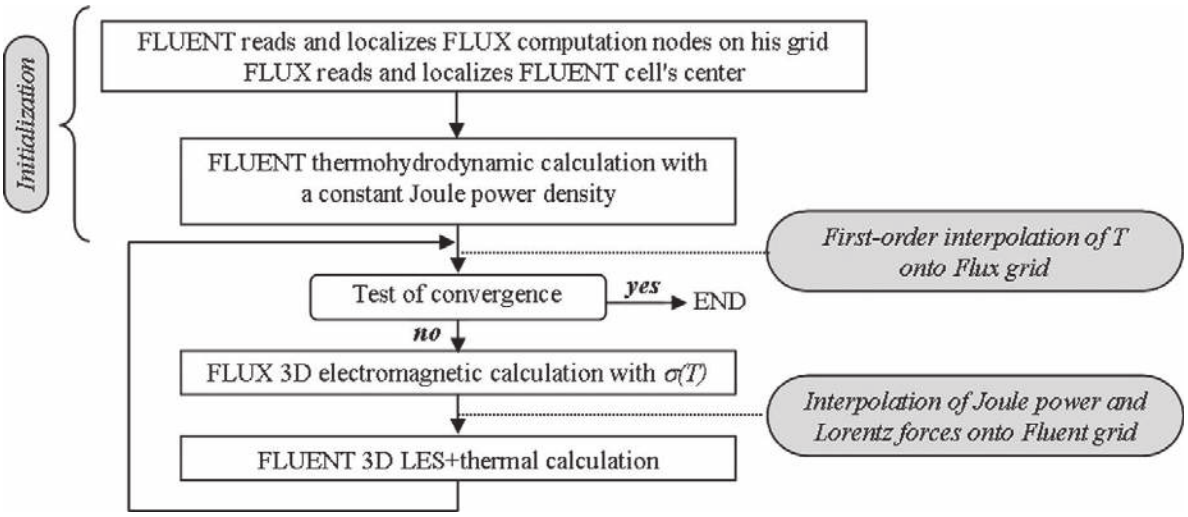

Fig. 2. Iterative algorithm for the Flux-Fluent coupling.

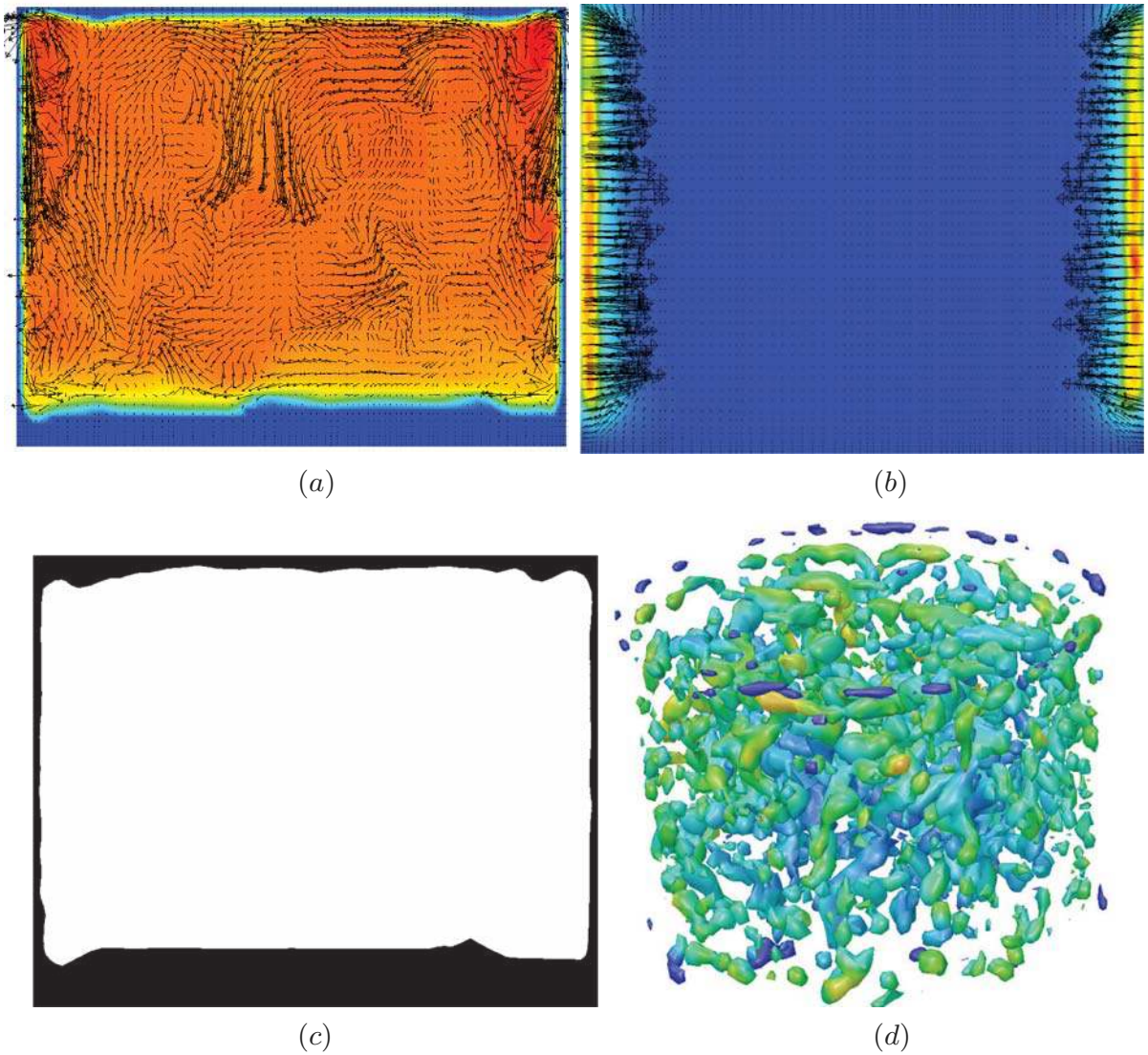

(*a*) (*b*)

(*c*) (*d*)

Fig. 3. Some typical results obtained after global thermal stabilization. (*a*) Temperature (range 2800–3277 K) and velocity vectors ($V_{\max} = 0.03$ m/s). (*b*) Joule power (Max: 7662 Wm^{-3}) and Lorentz forces vectors (Max: 6400 Nm^{-3}). (*c*) Crust profile defined by viscosity (black: solid, white: liquid). (*d*) Iso-contours of Q-criterion.

The temperature field, the velocity vectors, the Joule power density distribution and the viscosity are shown on a vertical cut plane. A 3D view of the iso-value of the Q-criterion is also shown, it helps to see the turbulence strutures (vortices) in the liquid part of the domain. The flow behaviour exhibits a quite well-developed turbulence resulting in a homogeneous temperature in the molten part of the load despite of the concentration of the Joule power density in the peripheral zone of the load due to the skin effect. The crust thickness along the vertical wall or bottom wall is clearly different. This thickness is of great interest to determine the ability of pouring.

3. Conclusions. The behavior of a large load of UO_2 melted in a cold crucible induction furnace has been numerically investigated. The simulation includes turbulence modelling coupled with induction modelling by the Lorentz forces, whereas Joule power density acts as a source term in the thermal equation. Such simulations are achieved in the Plinius-2 project in order to assist the sizing and conception of the future furnace. Further work is necessary to take into account the thermal resistance beween the skull layer and the crucible.

Acknowledgements. The authors thank Prof. S. Bechta (KTH Engineering Sciences, Sweden), Dr. D. Lopukh (LETI, St.-Petersburg, Russia) and G. Lecomte (ECM Technology, Grenoble, France) for their scientific support and collaboration.

References

[1] S. Hong, B. Min, J. Song, and H. Kim. Application of cold crucible for melting of UO_2/ZrO_2 mixture. *Materials Science and Engineering: A*, vol. 357 (2003), no. 12, pp. 297–303.

[2] B. Min, *et al.* Phase separation of metal-added corium and its effect on a steam explosion. *Journal of Nuclear Materials*, vol. 377 (2008), no. 3, pp. 458–466.

[3] S. Bechta, *et al.* Experimental studies of oxidic molten corium-vessel steel interaction. *Nuclear Engineering and Design*, vol. 210 (2001), no. 13, pp. 193–224.

[4] V. Asmolov, *et al.* Main results of study on the interaction between the corium melt and steel in the VVER-1000 reactor vessel during a severe accident performed under the MASCA project. *Physics of Atomic Nuclei*, vol. 73 (2010), no. 14, pp. 2301–2318.

[5] L. Jacoutot, *et al.* Strategy of coupling to model physical phenomena within molten glass bath heated by direct induction. *COMPEL*, vol. 27 (2008), no. 2, pp. 369–376.

[6] E. Sauvage, *et al.* Thermoconvective flow of molten glass heated by direct induction in a cold crucible. *Magnetohydrodynamics*, vol. 45 (2009), no. 4, pp. 535–542.

[7] S. Spitans, E. Baake, A. Jakovics, and H. Franz. Numerical simulation of electromagnetic levitation in a cold crucible furnace. *Magnetohydrodynamics*, vol. 51 (2015), no. 3, pp. 567–578.

[8] IAEA. *Thermophysical properties database of materials for light water reactors and heavy water reactors*, vol. IAEA-TECDOC-1496 (IAEA, 2006).

[9] J.L. Bates, C.A. Hinman, and T. Kawada. Electrical conductivity of uranium dioxide. *Journal of the American Ceramic Society*, vol. 50 (1967), no. 12, pp. 652–656.

[10] J. Smagorinsky. General Circulation Experiments with the Primitive Equations. *Monthly Weather Review*, vol. 91 (1963), p. 99.